



ISSN NO. 2320-5407

Journal homepage: <http://www.journalijar.com>

INTERNATIONAL JOURNAL
OF ADVANCED RESEARCH

RESEARCH ARTICLE

ROBOTIC CONFIGURATION FOR PARALYZED SWING LEG WITH EFFORT MINIMIZATION OF STANCE HIP TORQUES

A. Chennakesava Reddy¹, B. Kotiveerachari², P. Rami Reddy³

1. Professor, Department of Mechanical Engineering, JNTUH College of Engineering, Kukatpally, Hyderabad – 500 085, Telangana, India

2. Professor, Department of Mechanical Engineering, National Institute of Technology, Warangal, Telangana, India

3. Former Registrar, JNT University, Kukatpally, Hyderabad – 500 085, Telangana, India.

Manuscript Info

Manuscript History:

Received: 15 January 2015

Final Accepted: 22 February 2015

Published Online: March 2015

Key words:

Robot, paralyzed leg, pelvis, treadmill, walking motion.

*Corresponding Author

A. Chennakesava Reddy

Abstract

This research work was aimed at an alternate approach for walking and training the paralyzed leg with a robot attached to the pelvis. The dynamic properties considered in this work were mass, center of gravity, moments of inertia of each link and the friction at each joint. The least square method was employed to identify the dynamic properties after exciting the robot and collecting the data of joint positions, velocities, accelerations and applied forces. A robot attached to the pelvis was employed to control the stepping motion of a paralyzed person suspended on a treadmill. In this configuration, the twisted pelvis was able to pump required energy to the paralyzed leg. The collision of leg with ground was prevented by lifting the swing hip.

Copy Right, IJAR, 2015,. All rights reserved

INTRODUCTION

Human walking is a smooth, highly coordinated, rhythmical movement by which the body moves step by step in the desired direction. Damage in walking ability is frequent after the heart attack and spinal cord injury. The clinical stepping motion training is too little because the training is labor concentrated. Many therapists are obligatory to control the pelvis and legs. Body weight supported (BWS) training has shown assurance in enhancing walking after spinal cord injury as stated by Wickelgren (1998). The technique involves suspending the patient above a treadmill to partly relieve the body weight, and physically supporting the legs and pelvis while moving in a walking pattern. Patients who be given this therapy can considerably increase their independent walking ability (Barbeau et al., 1998; Ko and Badler., 1993). This technique works by force, position, and touch sensors in the legs during stepping in a repetitive manner, and that the circuits in the nervous system learn from this sensor input to generate walking style. Kinematic approaches for simulating human walking have been illustrated by various researchers over the years (Boulic et al., 1990; Calvert and Chapman., 1982; Reddy et al., 2004).

A difficulty in automating BWS training is that the required amount of forces at the pelvis and legs are unknown. In the field of computer animation, because of the complex hierarchical structure of the human being, most of the research in motion control of human beings has been devoted to ways of reducing the amount of specification necessary to achieve a desired motion. Bruderlin and Calvert (1993) have proposed procedural animation techniques to animate personalized human locomotion. In their system, three locomotion parameters, step length, step frequency and velocity, are used to specify the basic locomotion stride. Then, additional locomotion attributes are added at different levels of the motion control hierarchy to individualize the locomotion. Phillips and Badler (1993) have implemented an inverse kinematics algorithm to generate motions. Minimization of energy described by the constraints is used to choose the set of joint angles among the multiple inverse kinematics solutions. Hodgins et al. (1995) have introduced a dynamic approach to animate human running. The control algorithm is based on a cyclic state machine, which determines the proper control actions to calculate the forces, and

torques that satisfy the requirements of the task and input from the user.

The BWS training with robotics is an attractive as it improves the training. This article aims at an alternate approach toward generating strategy for developing dynamic motion planning for walking and training the paralyzed leg with a robot attached to the pelvis. The robotic configuration is swing leg with effort minimization of all joints. This configuration is studied to determine a practical gait trajectory using the optimization technique. The robot configuration as shown in figure 1 is used to assist the paralyzed leg and to simulate the walking pattern of the normal leg.

1 REHABILITATION ROBOT CONFIGURATION

Basically, all normal people walk in the same way. From human gait observations (Murray et al., 1964), the differences in gait between one person and another occur mainly in movements in the coronal and transverse planes. While walking, the position and orientation of legs change as shown in figure 2. In consequence, the rehabilitation robot configuration is defined by the author in his research work (2007). The rehabilitation robot is described kinematically by giving the values of link length, link twist, joint distance and joint angle. The rehabilitation robot transformation matrices are very vital for the dynamic analysis.

2 METHODOLOGY

The position and orientation of frame i relative to that of frame $(i-1)$ are given by

$$T_{0,n}(q_1, q_2, \dots, q_n) = T_{0,1}(q_1) T_{1,2}(q_2) \dots T_{n-1,n}(q_n) \quad (1)$$

where q_i is the joint variable for link i .

The mapping between the joint velocities and the end-effector velocities is defined by the differential kinematics equation

$$V_e = \begin{bmatrix} \omega_e \\ v_e \end{bmatrix} = J_e(q) \dot{q} \quad (2)$$

where V_e is the spatial velocity of the end-effector; w_e and v_e the angular and linear velocities of the end-effector, respectively; \dot{q} the generalized velocity of the robot manipulator; and J_e the Jacobian matrix. The Jacobian can be expressed entirely in terms of the joint screws mapped into the base frame. Each column of $J_e^s(q)$ depends only on q_1, q_2, \dots, q_{i-1} . In other words, the contribution of the i^{th} joint velocity to the end-effector velocity is independent of the configuration in the manipulator. The instantaneous spatial velocity of the end-effector is given by the twist

$$V_e^s = (\dot{T}_{0,n} T_{0,n}^{-1})^v = J_e^s(q) \dot{q} \quad (3)$$

where $J_e^s \in \mathfrak{R}^{6 \times n}$ is called the spatial Jacobian.

The spatial Jacobian can be expressed entirely in terms of the joint screws mapped into the base frame

$$J_e^s(q) = [Ad_{T_{0,1}} S_1 Ad_{T_{0,2}} S_2 \dots Ad_{T_{0,n}} S_n] \quad (4)$$

Each column of $J_e^s(q)$ depends only on q_1, q_2, \dots, q_{i-1} . In other words, the contribution of the i^{th} joint velocity to the end-effector velocity is independent of the later configuration in the manipulator. The body Jacobian J_e^b is defined by the relationship

$$V_e^b = (T_{0,n}^{-1} \dot{T}_{0,n})^v = \sum \left(T_{0,n}^{-1} \frac{\partial T_{0,n}}{\partial q_i} \right)^v \dot{q}_i = J_e^b(q) \dot{q} \quad (5)$$

The body Jacobian can be expressed as follows

$$J_e^b = [Ad_{T_{1,n}^{-1}} S_1 \quad Ad_{T_{2,n}^{-1}} S_2 \quad \dots \quad Ad_{T_{n-1,n}^{-1}} S_{n-1} S_n] \quad (6)$$

The body Jacobian can be expressed entirely in terms of the joint screws mapped into the end-effector frame. It maps the joint velocities into the corresponding spatial velocity of the end-effector in the end-effector frame. The spatial and body Jacobians are related by the adjoint transformation

$$J_e^s(q) = AD_{T_{0,n}} J_e^b \quad (7)$$

The dynamic equations of open-chained robot manipulators can be expressed in the general form

$$H(q)\ddot{q} + h(q, \dot{q}) = \tau \tag{8}$$

which relates the applied joint forces τ to the joint positions q and their time derivatives \dot{q} and \ddot{q} . $H(q)$ is the mass or inertia matrix and $h(q, \dot{q})$ contains the centrifugal, Coriolis, gravitational and frictional forces.

The Newton-Euler recursive algorithm of the inverse dynamics is as follows:

- Initialization

$$V_0, \dot{V}_0, F_{n+1} \tag{9}$$

- Forward recursion: $i = 1$ to n

$$V_i = Ad_{T_{i-1,i}} V_{i-1} + S_i \dot{q}_i \tag{10}$$

$$\dot{V}_i = Ad_{T_{i-1,i}} \dot{V}_{i-1} + S_i \ddot{q}_i + ad_{v_i} S_i \dot{q}_i \tag{11}$$

- Backward recursion: $i = n$ to 1

$$F_i = Ad_{T_{i-1,i}}^* F_{i+1} + J_i \dot{V}_i - ad_{v_i}^* + J_i \dot{V}_i - ad_{v_i}^* J_i V_i \tag{12}$$

$$\tau_i = S_i^T F_i + f_{ci} \text{sgn}(\dot{q}_i) + f_{vi} \dot{q}_i \tag{13}$$

In this algorithm, the index i represents the i^{th} link frame counted from the base frame ($i = 0$). The joint screw, spatial velocity, spatial acceleration and spatial force are written as S, V, \dot{V} and $F \in se(3)$, respectively. Particularly, V_0 and \dot{V}_0 represent the spatial velocity and acceleration of the base, respectively, while F_{n+1} represents the external spatial force on the last link or end-effector. $T_{i-1,i} \in SE(3)$ denotes the transformation from the $(i - 1)^{th}$ link frame to the i^{th} link frame. The joint velocity, acceleration, force and the Coulomb and viscous frictions are written as $\dot{q}, \ddot{q}, \tau, f_c$ and $f_v \in \mathfrak{R}$, respectively. And J is the spatial inertia matrix

$$J_i = \begin{bmatrix} I_i - m_i \hat{r}_i^2 & m_i \hat{r}_i \\ -m_i \hat{r}_i & m_i \bullet 1 \end{bmatrix} \tag{14}$$

where m_i and I_i are the mass and inertia of the i^{th} link, respectively; r_i is a vector from the origin of the i^{th} link frame to the center of mass of i^{th} link; \hat{r}_i is the skew symmetric matrix formed by r_i using the notation from the last chapter; and 1 is an identity matrix. The spatial velocity and force are

$$V_i = \begin{bmatrix} w_i \\ v_i \end{bmatrix} \text{ and } F_i = \begin{bmatrix} m_{ti} \\ f_{ti} \end{bmatrix} \tag{15}$$

where w, v, m_t and f_t are the angular velocity, linear velocity, moment and force, respectively. This recursive formulation shows how the spatial velocity and acceleration propagate forwards from the base to the end-effector and how the spatial force propagates backwards from the end-effector to the base.

Featherstone's (1988) articulated-body method supplies an efficient solution to the forward dynamics problem. Featherstone has shown that the equations of motion of each link can be expressed as follows:

$$F_i = \hat{J}_i \dot{V}_i + \hat{F}_i \tag{16}$$

where \hat{J}_i is the articulated-body inertia of link i , and \hat{F}_i is the bias force associated with link i . It is assumed that a spatial force F_{n-1} is applied to the articulated body. From the Newton-Euler recursive algorithm, it follows the equations of motion of each link

$$F_n = J_n V_n - ad_{v_n}^* J_n V_n \tag{17}$$

$$F_{n-1} = Ad_{T_{n-1,n}}^* F_n + J_{n-1} \dot{V}_{n-1} - ad_{v_{n-1}}^* J_{n-1} V_{n-1} \tag{18}$$

The articulated-body method can be applied to solve not only the forward dynamics but also the inverse dynamics.

In the present work, the hybrid dynamics problem was defined as a system of equations for articulated bodies in which either the applied force or the joint acceleration for each joint was known.

The hybrid dynamics algorithm is as follows:

- Initialization

$$V_0, \dot{V}_0, F_{n+1}, F_{b_{n+1}} = F_{n+1}, \hat{J}_{n+1} = 0, \hat{J}_{b_{n+1}} = 0, b_{n+1} = 0 \tag{19}$$

- Forward recursion: $i = 1$ to n

$$V_i = Ad_{T_{i-1,i}^{-1}} V_{i-1} + S_i \dot{q}_i \quad (20)$$

- Backward recursion $i = n$ to 1

$$\hat{J}_i = J_i + Ad_{T_{i,i+1}^{-1}}^* J_{b_{i+1}} Ad_{T_{i,i+1}^{-1}} \quad (21)$$

$$\hat{F}_i = -ad_{V_i}^* J_i V_i + Ad_{T_{i,i+1}^{-1}}^* (F_{b_{i+1}} + \hat{J}_{i+1} S_{i+1} b_{i+1}) \quad (22)$$

$$F_{b_i} = \hat{F}_i + \hat{J}_i ad_{V_i} S_i \dot{q}_i \quad (23)$$

$$J_{b_i} = \begin{cases} \hat{J}_i & i \in I^a \\ \hat{J}_i - \hat{J}_i S_i S_i^T \hat{J}_i / S_i^T \hat{J}_i S_i & i \in I^p \end{cases} \quad (24)$$

$$b_i = \begin{cases} \ddot{q}_i & i \in I^a \\ (\tau_i - S_i^T F_{b_i}) / S_i^T \hat{J}_i S_i & i \in I^p \end{cases} \quad (25)$$

- Forward recursion: $i = 1$ to n

$$\begin{cases} \tau_i = S_i^T (F_{b_i} + \hat{J}_i Ad_{T_{i-1,i}^{-1}} \dot{V}_{i-1} + \hat{J}_i S_i b_i) & i \in I^a \\ \ddot{q}_i = b_i - \left(S_i^T \hat{J}_i Ad_{T_{i-1,i}^{-1}} \dot{V}_{i-1} \right) / \left(S_i^T \hat{J}_i S_i \right) & i \in I^p \end{cases} \quad (26)$$

$$\dot{V}_i = Ad_{T_{i-1,i}^{-1}} \dot{V}_{i-1} + S_i \ddot{q}_i + ad_{V_i} S_i \dot{q}_i \quad (27)$$

The B-spline curve is used to the joint trajectories (Reddy, 2008). The B-spline curve, $q \in \mathfrak{R}$ is written as

$$q(t, p) = \sum_{j=0}^m p_j B_{j,k}(t) \quad (28)$$

where $p = \{p_0, \dots, p_m\}$, with p_j are the control points and $B_{j,k}$ is the B-spline basis function. The index k defines the order of the basis polynomial, e.g. $k = 4$ for a cubic one or $k = 6$ for a quintic one. The semi-infinite constraints are transformed into a set of linear inequalities by exploiting the convex hull property.

3 HUMAN MODEL AND WALKING MOTION

For studying the motion of the legs, the head, torso, pelvis, and arms were combined into a single rigid body (upper trunk). The walking gait cycle (figure 3) was assumed to be bilaterally symmetric (Reddy and Kotiveerachari, 2008). The left-side stance and swing phases were assumed to be identical to the right-side stance and swing phases, respectively. Thus, only one-half of the gait cycle was simulated in this study. The stance hip was modeled as a two degrees-of-freedom (DOF) universal joint rotating about the x - and y -directions. The upper trunk was fixed about the z -axis. The swing hip was modeled as a 3 DOF ball joint rotating about axes in the x -, y -, and z - directions. The knee and ankle were modeled as 1 DOF hinge joints about the z -axis.

Motion capture data of major body segments for an unimpaired person during treadmill walking was obtained using a video-based system at FESTO Pvt.Ltd, Bangalore. The frequency of motion capture was 50 Hz. External markers were attached to the body at the antero-superior iliac spines (ASISs), knees, ankles, tops of the toes, and backs of the heels (Reddy and Babu, 2011). The link lengths and joint orientations are shown in Table 1. The human subject was 1.95 m tall and weighed 70 kg. Passive torque-angle properties of the hip, knee, and ankle joints were measured for the subject with a Biodex active dynamometer. Joints were measured in a gravity-eliminated configuration. The dynamic properties of the human model are given in Table 2.

The joints were modeled as nonlinear springs in which the joint torque was a polynomial function of the joint angle. A least squares method was used to best-fit polynomials. Third order polynomial function was used for the torque-angle property of each joint. A polynomial of order 7 was used to the ankle joint data. The polynomial equations for curves are mentioned as follows:

Hip external/internal rotation (60⁰,60⁰)

$$\tau_m = 0.6837 - 0.7621q + 0.9772q^2 - 2.2620q^3 \tag{29}$$

Hip abduction/adduction (50⁰,30⁰)

$$\tau_m = 0.0542 - 0.8266q + 6.0205q^2 - 29.0271q^3 \tag{30}$$

Hip extension/flexion (35⁰,70⁰)

$$\tau_m = 1.0863 + 1.5721q + 6.3488q^2 - 23.0405q^3 \tag{31}$$

Knee flexion/extension (140⁰,0⁰)

$$\tau_m = 24.9343 - 53.1584q + 37.5211q^2 - 9.8685q^3 \tag{32}$$

Ankle plantar/dorsal flexion (-52⁰,46⁰)

$$\tau_m = 0.1305 - 3.99564q + 1.5596q^2 - 4.7881q^3 + 2.4229q^4 + 6.2372q^5 - 5.6802q^6 + 19.5304q^7 \tag{33}$$

In addition to the polynomial function, a nonlinear spring-damper system was used to place a hard limit on joint movement when it is close to its upper and lower bounds.

$$\tau_{sd} = \begin{cases} -\beta(10^4(q - q_2) + 5 \times 10^2 \dot{q}) & \text{if } q \geq q_2 \\ -\beta(10^4(q - q_1) + 5 \times 10^2 \dot{q}) & \text{if } q \leq q_1 \\ 0 & \text{otherwise} \end{cases} \tag{34}$$

$$\text{where } \beta = \begin{cases} 6 \times 10^5(q - q_2)^5 - 1.5 \times 10^5(q - q_2)^4 + 10^4(q - q_2)^3 & \text{if } q_2 + 0.1 \geq q \geq q_2 \\ -6 \times 10^5(q - q_1)^5 - 1.5 \times 10^5(q - q_1)^4 + 10^4(q - q_1)^3 & \text{if } q_1 - 0.1 \geq q \geq q_1 \\ 1 & \text{otherwise} \end{cases}$$

The function τ_{sd} is c^2 continuous in order to be used in the computation of the analytical gradient in the dynamic motion optimization. Four steps at three different treadmill walking speeds (1.75, 1.25 and 0.75 m/sec) were obtained from motion capture. The swing motion was considered to be an optimal control problem as follows:

$$\min_{\tau(t)} J_c = \frac{1}{2} \int_0^{t_f} \sum_{i=4}^{10} w_{ei} \tau_i^2 dt \tag{35}$$

$$\text{s.t. } H(q)\ddot{q} + h(q, \dot{q}) = \tau + \tau_{msd} \tag{36}$$

$$q(0) = q_0, \quad \dot{q}(0) = \dot{q}_0 \tag{37}$$

$$q(t_f) = q_f, \quad \dot{q}(t_f) = \dot{q}_f \tag{38}$$

where τ_1, τ_2 and τ_3 are the generalized forces associated with the translation of the stance hip (and are not included in the cost function since the position of the stance hip was specified by the motion capture data); τ_4 and τ_5 are the moments corresponding to the two rotations of the stance hip (controlled by the robot); τ_6, τ_7 and τ_8 are the swing hip moments (corresponding to hip abduction/adduction and extension/flexion, external/internal rotation, respectively); τ_9 and τ_{10} correspond to knee and ankle rotation moments, respectively; and w_{ei} 's are positive weighting coefficients. $\tau_6 \sim \tau_{10}$ were assumed zero for the impaired leg. $\tau_{msd4} \sim \tau_{msd10}$ were modeled as nonlinear spring-damper muscle systems while $\tau_{msd1} \sim \tau_{msd3}$ were zero since no muscular force is needed for the linear translation of the stance hip.

4 RESULTS AND DISCUSSION

The joint positions are shown in figure 4 & 5. Solid lines represent the simulated data. The dashed lines signify

experimental data. The swing hip, knee and ankle joints were made passive to simulate a paralyzed person. 8 parameters for each active joint) were used in the optimization. This configuration was modeled with both active and passive joints. The total optimization time was 2 hours 45 minutes.

The joint motions of the gait for duration 0.45 sec and 0.60 sec are respectively shown in figure 6 & 7. Solid lines represent the simulated data. The dashed lines signify experimental data. For the duration 0.45 sec, the simulated joint motions of the gait are higher than the experimental data. This might be due to lifting swing hip. For the duration 0.60 sec, the simulated joint motions of the gait are lower than the experimental data. This might be owing to over twisting of pelvis. In this configuration the swing hip was lifted to avoid the collision between the legs and between the swing leg and the ground. The pelvis was twisted to pump energy into the paralyzed leg. The leg was moved to get the desired motion to the paralyzed leg. Therefore, this configuration was able to provide a strategy of motion that could achieve repetitive stepping by shifting the pelvis alone. The torques of the joints are shown in figure 8. The torques obtained from the simulation were observed to be the same pattern of variation for gait durations of 0.45 sec and 0.60 sec. But, the simulated torques were oscillatory due to lifting of swing hip and twisting of pelvis than the experimentally determined. This is also due to minimum number of motion data-capture points to record experimental data.

Reddy, A.C., and Babu, G.S. (2011): Dynamic mechanisms of kneecap, compliant ankle and passive swing leg to simulate human walking robot, *Int. J. Adv. Mechatro. Robo.*, 3(1):1-7.

Wickelgren, I. (1998): Teaching the spinal cord to walk. *Sci.* 279(1):319–321.

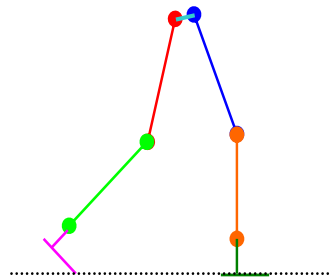


Figure 1: Rehabilitation robot to represent normal legs.

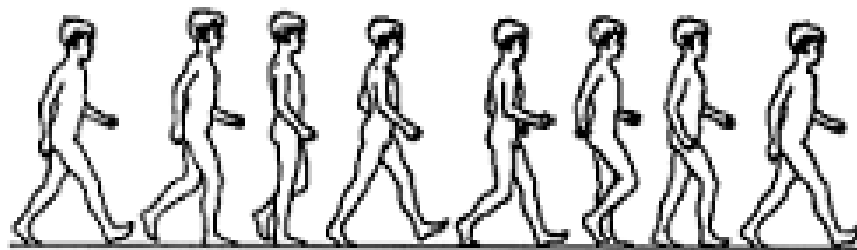


Figure 2: Change of position and orientation of legs during walking

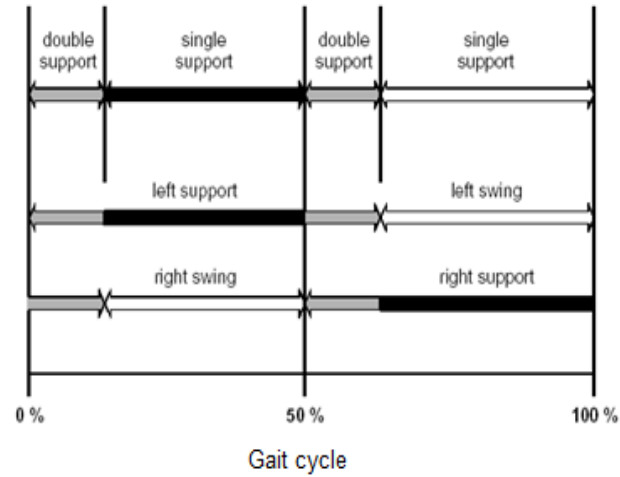


Figure 3: Gait cycle of human walking

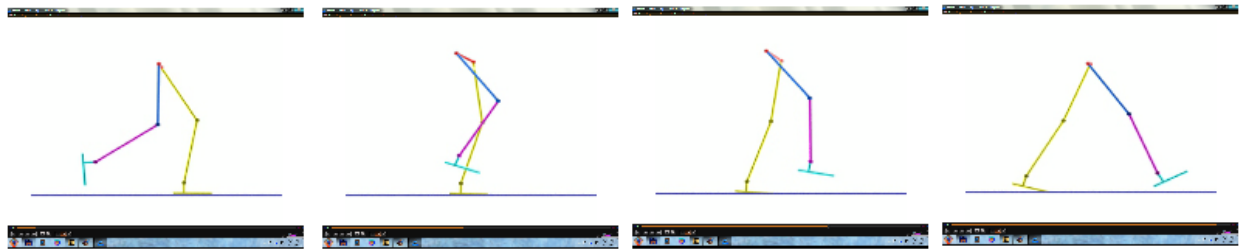
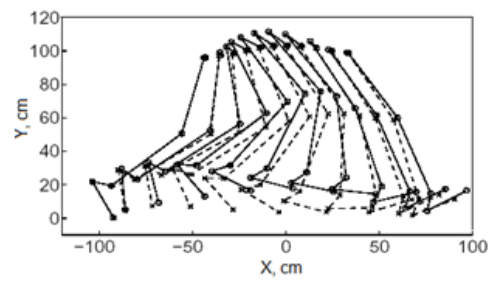


Figure 4: Gait for duration of 0.45 sec

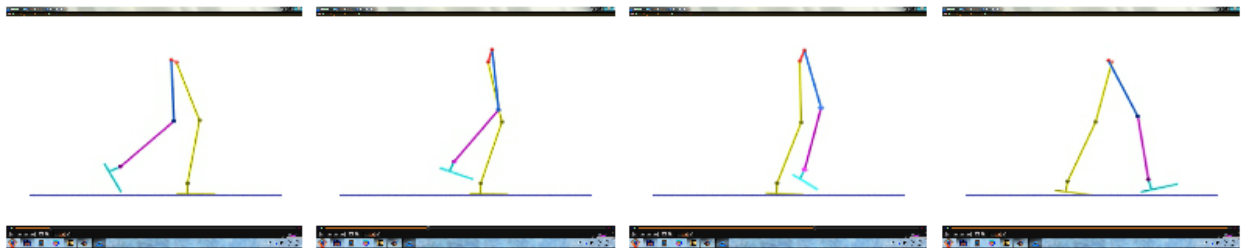
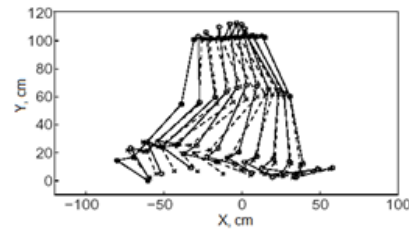


Figure 5: Gait for duration of 0.60 sec

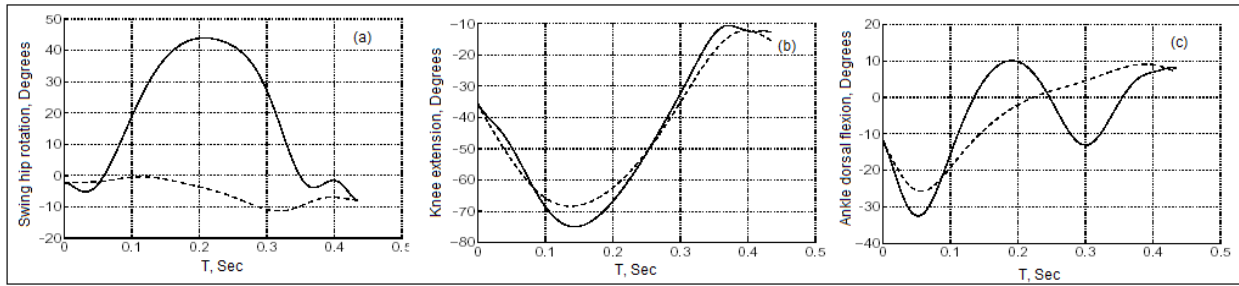


Figure 6: The joint motions (duration 0.45 sec).

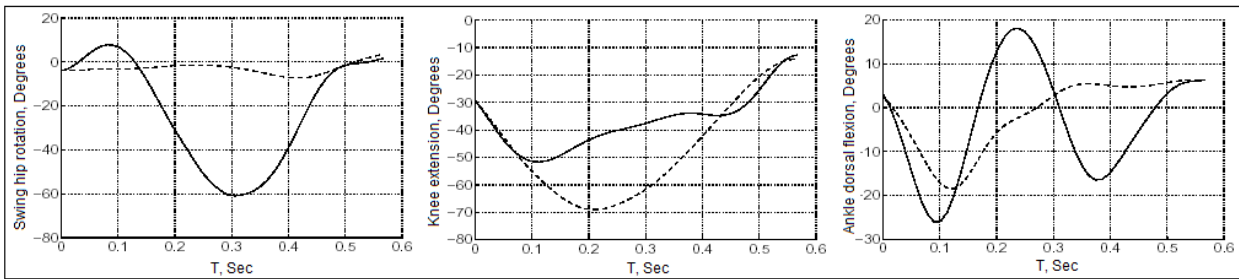


Figure 7: The joint motions (duration 0.60 sec).

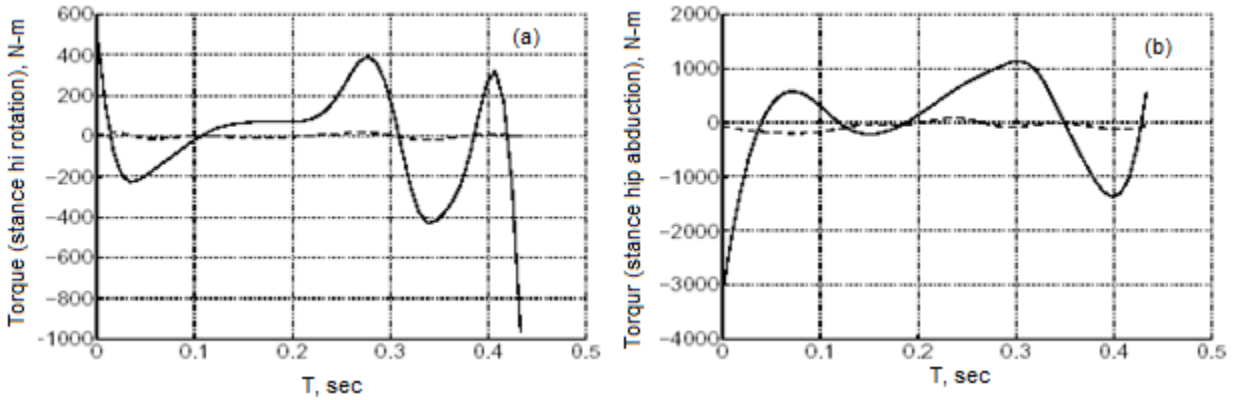


Figure 8. Joint torques (for duration of 0.45 sec)

TABLE 1: Link Lengths

l_{hip}	$l_{upperleg}$	$l_{lowerleg}$	l_{foot}	l_{toe}	l_{heel}
0.15 m	0.47 m	0.49 m	0.08	0.18 m	0.07 m

TABLE 2: Dynamic Properties of Human Model

Link	Mass, Kg	Inertia, Kg-m ²	Center of Mass, m

Upper Trunk	46.05	$\begin{bmatrix} 3.23 & 0 & 0 \\ 0 & 0.78 & 0 \\ 0 & 0 & 2.76 \end{bmatrix}$	$\begin{Bmatrix} -0.001 \\ 0.360 \\ 0 \end{Bmatrix}$
Upper Leg	9.54	$\begin{bmatrix} 30.16 & 0 & 0 \\ 0 & 0.035 & 0 \\ 0 & 0 & 1.15 \end{bmatrix}$	$\begin{Bmatrix} -0.025 \\ -0.170 \\ 0.007 \end{Bmatrix}$
Lower Leg	3.56	$\begin{bmatrix} 0.064 & 0 & 0 \\ 0 & 0.006 & 0 \\ 0 & 0 & 0.062 \end{bmatrix}$	$\begin{Bmatrix} -0.005 \\ -0.207 \\ 0.019 \end{Bmatrix}$
Foot	1.44	$\begin{bmatrix} 0.003 & 0 & 0 \\ 0 & 0.009 & 0 \\ 0 & 0 & 0.007 \end{bmatrix}$	$\begin{Bmatrix} 0.044 \\ -0.040 \\ 0.010 \end{Bmatrix}$

CONCLUSIONS

Walking motion was generated for a robot attached to the pelvis of a paralyzed person suspended on a treadmill. A leg swing motion was created by lifting swing hip and twisting of pelvis. The twisted pelvis was able to pump energy into the paralyzed leg. The collision of leg with ground was prevented by lifting swing hip.

REFERENCES

Barbeau, H., Norman, K., Fung, J. J., Visintin, J., and Ladoucer, M. (1998): Does neuro-rehabilitation play a role in the recovery of walking in neurological populations. *Ann. N.Y. Acad. Sci.*, 860:pp.377–392.

Boulic, N., Thalmann M., and D. Thalmann. (1190): A Global Human Walking Model with Real- time Kinematic Personification, *Visual Comput.*, (6): 344-358.

Bruderlin, A. and Calvert, T. W. (1993): Interactive Animation of Personalized Human Locomotion. *GI'93*, 28: 17-23.

Calvert T.W., and Chapman, J. (1982): Aspects of the kinematic simulation of human movement. *IEEE Comput. Graph. Appl.*, 2(9): 41-50.

Featherstone, R. (1988): *Robot Dynamics Algorithms*, Kluwer Academic Publishers, Norwell, MA.

Hodgins, J.K., Wooten, W.L., Brogan, A.C., and O'Brien, J.F. (1995): Animating Human Athletics. *Comput. Graph.*, .29:71-78.

Ko, H. and Badler, N.I. (1993): Straight-line walking animation based on kinematic generalization that preserves the original characteristics. *GI'93*, 28: 9-16.

Murray, M. P., Drought, A. B., and Kory, R. C. (1964): Walking patterns of normal men. *J. Bone Joint Surg.*, 46A:335-359.

Phillips, C.B., Badler, N. I., and Webber, B. L. (1993): *Simulating humans*. Oxford University Press.

Reddy, A.C., Kotiveerachari, B., and .Reddy, P.R (2004): Dynamic trajectory planning of robot arms, *J. Manuf. Technol.*, 3(3):15-18.

Reddy, A.C. (2007): Studies on synthesis and optimization of robotic configurations used for training of paralyzed person through dynamic parameter consideration. Ph.D Thesis.

Reddy, A.C., (2008): *CAD/CAM: Concepts and Applications*. PHI Learning Private Limited, New Delhi.

Reddy, A.C., and Kotiveerachari, B. (2008): Different methods of robotic motion planning for assigning and training paralysed person, *J.Inst. Eng.*, 88(2): 37-41.